Active control of kink modes using a non-magnetic, extreme ultraviolet sensor array

J.P. Levesque[1], J.W. Brooks[1,2], S. DeSanto[1], M.E. Mauel[1], G.A. Navratil[1]

[1] *Dept. of Applied Physics and Applied Math., Columbia University, New York, NY, USA*

[2] *Naval Center for Space Technology, US Naval Research Laboratory, Washington DC, USA*

1. Introduction

Instability control in tokamaks often utilizes arrays of magnetic sensors and actuators positioned near the plasma edge and behind plasma facing components. Placing magnetic coils behind thick shielding walls would improve their longevity in a reactor at the expense of reducing frequency response, while a light-based detector could still respond quickly and with enhanced spatial sensitivity. We report the first demonstration of active feedback control of kink modes using non-magnetic sensors consisting of extreme ultraviolet (EUV) detector arrays as input to drive a set of magnetic control coils in real time. Suppression and amplification of $m/n = 3/1$ kink modes on the HBT-EP tokamak [1] are observed as a function of the applied feedback phase angle relative to the measured EUV emissivity fluctuations.

2. HBT-EP diagnostic and control system

An overview of the HBT-EP EUV mode control sensors and actuators is shown in Figure 1. Four AXUV16 diode arrays each provide 16 views of the poloidal cross section. 100nm-thick Al filters are used in front of each array to block visible light, and admit EUV/SXR photons with energies above 15eV. Transimpedance amplifiers having gains of 50k-400k convert the photocurrent to voltage, which is then routed to the control system's input digitizer. The feedback input digitizer, control algorithm, and actuators are identical to the system previously reported in [2]. The only software differences in the controller are that the input projection matrix has been changed to accommodate the EUV inputs with their relevant mode geometry,

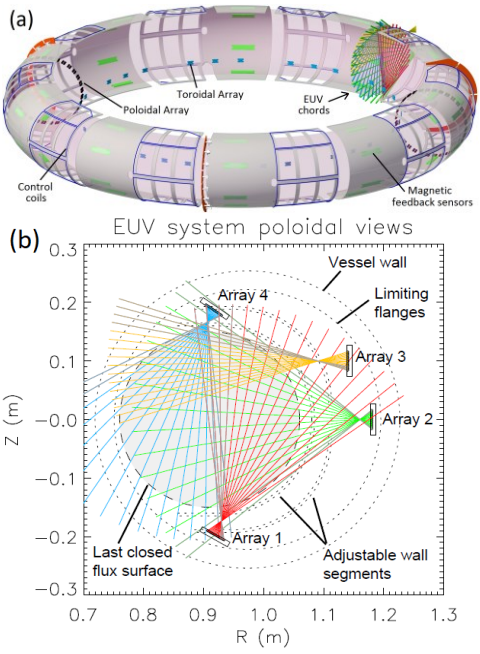

Figure 1: a) Overview of the HBT-EP EUV control system, and b) Poloidal layout of the EUV chords. The 48 chords shown in colour are used for feedback, while the 16 grey chords are excluded.

and the output matrix is updated to expand the tracked states onto the control coils for the magnetic mode geometry in this study. A D-tAcq ACQ196 analog input digitizer transfers data to the feedback system at 166kSps, while another ACQ196 digitizer records the data at 500kSps for offline analysis.

In-vessel saddle coils apply radial fields using a pattern that couples well to the targeted 3/1 modes. The total latency from light detection to application of requested fields on the plasma surface is about 22 μs.

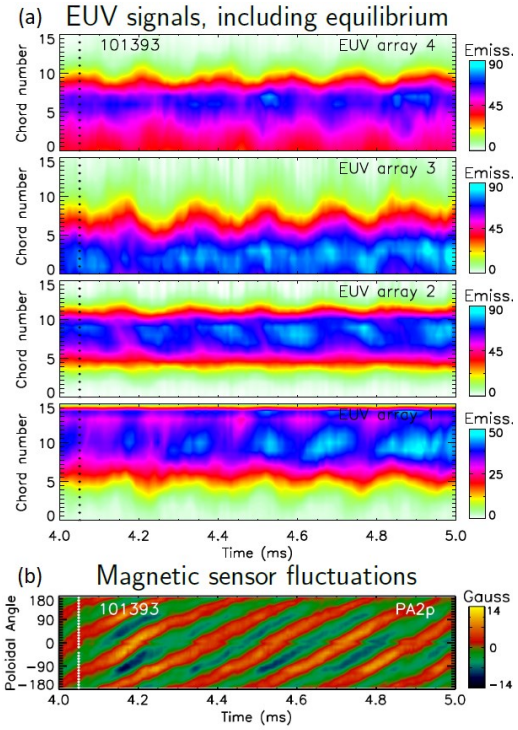

Figure 2: Contour plots of a) EUV and b) magnetic measurements from mode activity in shot 101393, the baseline feedback-off discharge used to establish the mode tracking basis set. EUV plots show the full signal of the four arrays including equilibrium, while the magnetic plot has the equilibrium removed.

3. Kink mode reference discharge

A reference discharge without feedback was used to generate the EUV basis vectors for projecting the mode measurements during feedback. An $m/n = 3/1$ kink mode was measured while the edge safety factor was near 2.6 during a positive plasma current ramp which maintained the instability drive via a broad current profile. Example EUV data and magnetic fluctuations from a poloidal array of poloidal field sensors for the target period are shown in Figure 2. A 3/1 mode rotating at 6 kHz is evident from the magnetic fluctuations, with corresponding fluctuations in the EUV data. Forty-eight EUV chords having good response to modes from the target discharge were selected to use for the real-time mode tracking; these chords are indicated as coloured lines in Figure 1. The remaining edge chords had a poor signal-to-noise ratio for this study, which has since been resolved by improving the diagnostic grounding scheme.

Singular Value Decomposition (SVD) is used to analyse the data to extract dominant mode features [3, 4]. Defining a matrix of fluctuating EUV data versus time as $S = U\Sigma V^{\dagger}$ yields two prominent temporal modes (chronos) within the columns of U, along with their spatial modes (topos) within the rows of $V^{\dagger}$ corresponding to quadrature bases of an $n = 1$ mode. Defining the plasma mode's amplitude as $A(t) = \sqrt{(\sigma_a \vec{u}_a(t))^2 + (\sigma_b \vec{u}_b(t))^2}$ and

phase as $\phi(t) = \mathrm{atan}(\sigma_b \vec{u}_b(t)/\sigma_a \vec{u}_a(t))$, where $\vec{u}_i(t)$ are the projections of the data onto each of the SVD bases, allows tracking of mode dynamics for the feedback system. This basis set uses no *a priori* prescription for the poloidal mode structure as would be imposed from e.g. a synthetic diagnostic. This amplitude and phase definition also allows direct comparison with dynamics measured using magnetic sensors, to within an arbitrary phase offset and amplitude scale factor. The dominant spatial modes from analysing only the EUV data are shown in Figure 3(a). For comparison, the spatial modes obtained by analysing only magnetic sensors are shown in Figure 3(b). The magnetic modes have a clear $n = 1$ sinusoidal geometry with a phase-shifted "sine/cosine" pair, while the EUV mode signature is not as intuitive. Chords in EUV Array 4 yield a larger amplitude than the other EUV chords in the spatial modes in part due to differences in amplifier gains.

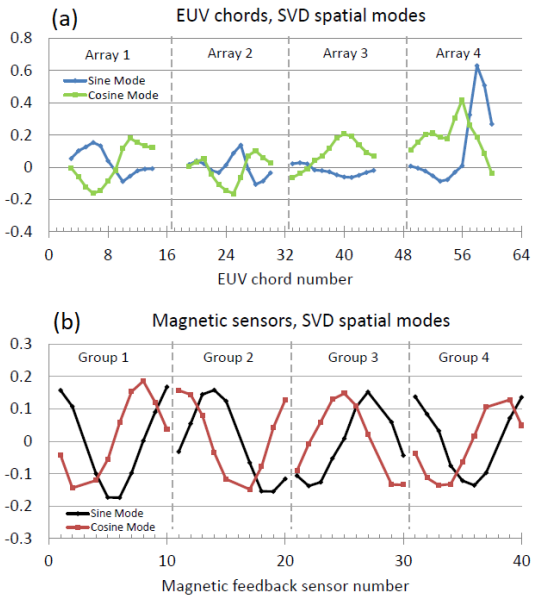

Figure 3: Two dominant SVD spatial modes from a) 48 chords of the EUV system and b) 36 poloidal field sensors from the magnetic feedback system.

Measured mode amplitude and phase versus time for EUV and magnetic sensors for this period are compared in Figure 4. The phases follow each other very well, while the EUV data show an extra amplitude modulation versus time which is not apparent in the magnetic data. This EUV amplitude modulation is likely due to the viewing chord geometry and basis set for this particular case; using different views or a modified basis set would likely remove or eliminate this modulation.

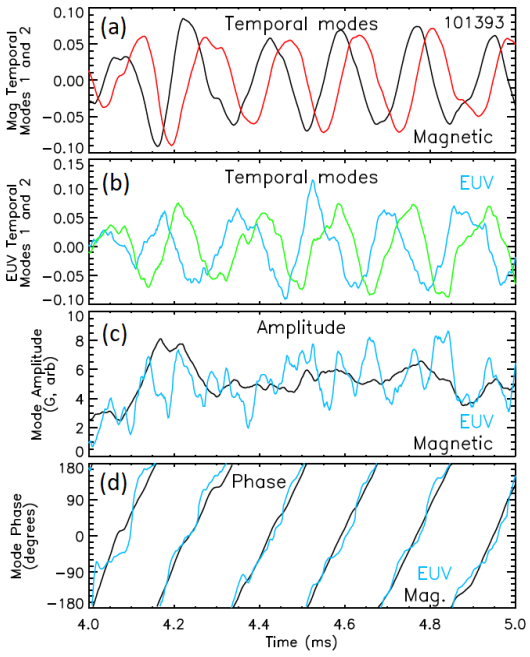

Figure 4: Comparison of modes from separately analysing a) magnetic data and b) EUV data, using appropriate SVD bases. Resulting amplitude and phase (c and d) agree well between the two diagnostics.

4. Feedback results

A feedback phase angle scan was completed for plasmas similar to the shot shown in Figure 2. The programmed phase shift between the detected and applied mode was adjusted between discharges, while the feedback gain remained the same. Resulting mode amplitudes versus programmed phase are shown in Figure 5. The feedback system was able to suppress the modes for phase angles around 225°, and amplify at phase angles around 0°. Phase scan results are qualitatively similar to phase scans using magnetic-only feedback [2]; mode amplification is seen roughly at opposite feedback phase angles compared to suppression.

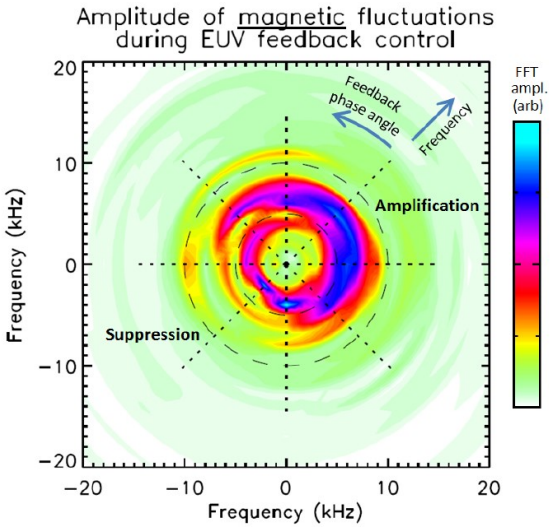

Figure 5: Compass scan of feedback results versus feedback phase angle. Mode suppression is seen at feedback phase angles near 225°.

Results here represent the first feedback run of this system using the EUV inputs. There is room for improvement by changing the feedback algorithm or tracked EUV basis states. Ongoing experiments include using the system for real-time tomographic reconstructions in the feedback loop for mode control and equilibrium position control.

Acknowledgements

This work is supported by U.S. Department of Energy, Office of Science, Office of Fusion Energy Sciences, Grant DE-FG02-86ER53222.

References

[1] Maurer D.A. *et al*., Plasma Physics and Controlled Fusion **53** 074016 (2011)

[2] Peng Q. *et al*., Plasma Physics and Controlled Fusion **58** 045001 (2016)

[3] Dudok de Wit T. *et al*., Physics of Plasmas **1** 3288 (1994)

[4] Levesque J.P. *et al*., Nuclear Fusion **53** 073037 (2013)